Comparison of Model-simulated Atmospheric Carbon Dioxide with GOSAT Retrievals

Changsub Shim*, Ray Nassar[1] and Jhoon Kim[2]

Korea Environment Institute, 290 Jinheung-ro, Eunpyeong-gu, Seoul, Korea
[1]Environment Canada, 4905 Dufferin St, Toronto, Ontario, Canada
[2]Department of Atmospheric Sciences, Yonsei University, 50 Yonsei-ro, Seodaemun-gu, Seoul, Korea

*Corresponding author. Tel: +81-2-380-7701, E-mail: marchell@gmail.com

ABSTRACT

Global atmospheric CO_2 distributions were simulated with a chemical transport model (GEOS-Chem) and compared with space-borne observations of CO_2 column density by GOSAT from April 2009 to January 2010. The GEOS-Chem model simulated 3-D global atmospheric CO_2 at $2° \times 2.5°$ horizontal resolution using global CO_2 surface sources/sinks as well as 3-D emissions from aviation and the atmospheric oxidation of other carbon species. The seasonal cycle and spatial distribution of GEOS-Chem CO_2 columns were generally comparable with GOSAT columns over each continent with a systematic positive bias of ~1.0%. Data from the World Data Center for Greenhouse Gases (WDCGG) from twelve ground stations spanning 90°S-82°N were also compared with the modeled data for the period of 2004-2009 inclusive. The ground-based data show high correlations with the GEOS-Chem simulation ($0.66 \leq R^2 \leq 0.99$) but the model data have a negative bias of ~1.0%, which is primarily due to the model initial conditions. Together these two comparisons can be used to infer that GOSAT CO_2 retrievals underestimate CO_2 column concentration by ~2.0%, as demonstrated in recent validation work using other methods. We further estimated individual source/sink contributions to the global atmospheric CO_2 budget and trends through 7 tagged CO_2 tracers (fossil fuels, ocean exchanges, biomass burning, biofuel burning, net terrestrial exchange, shipping, aviation, and CO oxidation) over 2004-2009. The global CO_2 trend over this period (2.1 ppmv/year) has been mainly driven by fossil fuel combustion and cement production (3.2 ppmv/year), reinforcing the fact that rigorous CO_2 reductions from human activities are necessary in order to stabilize atmospheric CO_2 levels.

Key words: Atmospheric CO_2, GEOS-Chem, GOSAT CO_2, WDCGG

1. INTRODUCTION

Understanding the global atmospheric CO_2 distribution and budget are important for achieving CO_2 emission reduction targets in the 21st century. However, the large uncertainties in CO_2 biospheric fluxes make it difficult to gauge the pathways of human-made CO_2 emissions within the Earth's system. Recently, there has been growing interest in the global atmospheric CO_2 budget and space-borne measurements of the global CO_2 distribution (Kulawik *et al.*, 2010; Crevoisier *et al.*, 2009; Yokota *et al.*, 2009; Chahine *et al.*, 2008; Buchwitz *et al.*, 2007) are contributing to our understanding of the topic. The current effort of global CO_2 monitoring from space has increased the possibility of constraining CO_2 fluxes from the natural sectors such as terrestrial vegetation and the ocean, since the satellite monitoring can give better spatial coverage than ground-based observations. Past studies have used satellite observations of CO_2 for constraining fluxes with varying degrees of success (Nassar *et al.*, 2011; Chevallier *et al.*, 2009, 2005), owing to the limited information on CO_2 near the Earth's surface provided by the thermal-infrared satellite measurements used.

In January 2009, the Greenhouse gases Observing Satellite (GOSAT) was launched and has observed carbon dioxide (CO_2) and methane (CH_4) distributions since April 2009 with good observational sensitivity to these gases near the surface. The main objective of the GOSAT project is to reduce the uncertainties in the greenhouse gas (GHG) fluxes on a subcontinental basis, which can provide additional information to help improve predictions of future global warming (Maksyutov *et al.*, 2008).

In this study, we focused on the comparison of simulated global CO_2 by a 3-D global chemical transport model (GEOS-Chem) with the GOSAT retrievals from April 2009 and January 2010. To evaluate the model

performance we used ground-based CO_2 measurements from 12 stations, which enabled us to remove the model bias and better estimate the bias in GOSAT CO_2 observations. In addition, we estimated the contributions of each CO_2 source and sink to the global atmospheric CO_2 budget for 6 years (from January 2004 and January 2010). The details of the GOSAT data and model simulation are explained in sections 2 and 3 and comparisons are described in section 4. The estimated source/sink contributions to global atmospheric CO_2 concentration are also discussed in section 4.

2. DATA

2.1 GOSAT CO_2 Products

GOSAT (also known as Ibuki), is the first successful satellite designed specifically to measure the concentrations of atmospheric carbon dioxide and methane (the two greenhouse gases making the largest contribution to climate change) with good sensitivity near the surface. GOSAT has a 666 km sun-synchronous orbit and completes one orbit in ~100 minutes providing global coverage in approximately 3 days (Kadygrov *et al.*, 2009). The GOSAT Thermal And Near-Infrared Sensor for carbon Observation (TANSO) consists of two units: the Fourier Transform Spectrometer (FTS) and the Cloud Aerosol Imager (CAI) (Kuze *et al.*, 2006). The TANSO-FTS has three bands in the Short Wave InfraRed (SWIR) region (0.76, 1.6, and 2.0 μm) and a wide Thermal Infrared (TIR) band (5.5-14.3 μm) with a circular ~10.5 km instantaneous field of view at nadir (Yokota *et al.*, 2009). The retrieval of greenhouse gases from FTS spectra excludes the cloudy pixels by screening using the images from CAI, which results in a significant reduction of data (Kadygrov *et al.*, 2009). The retrieved concentration is obtained from maximum a posteriori (MAP) method with a priori information from a radiative transfer model (RTM) and the pre-processed measured spectra. The overall retrieval algorithm for GOSAT CO_2 and CH_4 products is described at Yoshida *et al.* (2011, 2010).

We used the GOSAT CO_2 level 2 (L2) products from column abundance retrieved from Short Wave Infra-Red (SWIR) radiance spectra (version 01.1×) based on retrievals led by the National Institute for Environmental Studies (NIES). The details of the products including the retrieval processes and observation results are at http://www.gosat.nies.go.jp/index_e. html.

3. GEOS-CHEM MODEL

GEOS-Chem is a global chemical transport model that uses GEOS (Goddard Earth Observing System) assimilated meteorological fields from the NASA Global Modeling and Assimilation Office (GMAO). The most common application of this model includes O_x-NO_x-VOC chemistry and transport (Bey *et al.*, 2001). The first version of the GEOS-Chem CO_2 mode was developed by Suntharalingam *et al.* (2004), which included atmospheric CO_2 fluxes from biomass burning, biofuel burning, fossil fuel combustion and cement production, ocean exchange and terrestrial biospheric exchange. In this work, we applied the CO_2 update by Nassar *et al.* (2010), which improved the CO_2 flux inventories and added CO_2 emissions from international shipping and aviation (3D). This version also accounts for the chemical production of CO_2 from CO oxidation throughout the troposphere (Nassar *et al.*, 2010), a significant source of CO_2 (~1.05 Pg C/yr) that most other models count as surface emissions. In addition, use of the tagged tracer simulation, which considers each source/sink as an independent tracer, allows one to estimate the source/sink contributions to global atmospheric CO_2 concentration. The GEOS-Chem CO_2 module does not consider on-line full chemistry mechanisms (HO_x-NO_x-VOCs) to estimate CO_2 concentration. Instead, the CO_2 chemical production uses the monthly CO loss rate from an archived full chemistry run to represent CO_2 production (Nassar *et al.*, 2010), since CO oxidation is the primary pathway for atmospheric CO_2 production.

The CO_2 emissions from fossil fuel burning and cement manufacture were based on the inventory developed at the Carbon Dioxide Information and Analysis Centre (CDIAC) of the Oak Ridge National Laboratory (ORNL) with regional and seasonal variability that spans 1950-2007 (Andres *et al.*, 2011). However, this study only used the annual mean data since the monthly-varying inventory was not publicly available at the outset of this study. CO_2 emissions from fossil fuel combustion and cement production in the CDIAC inventory contributed 7.4-8.1 PgC/yr during the period of 2004-2007. The CO_2 emissions from biomass burning used year-specific Global Fire Emission Database version 2 (GFEDv2) (van der Werf *et al.*, 2006). The mean global annual CO_2 in GFEDv2 (1997-2008) is 2.35 PgC/yr. The biofuel burning CO_2 contribution used the annual mean inventory by Yevich and Logan (2003), with emissions of 0.80 Pg C/year. Terrestrial biospheric exchange is the most important CO_2 flux and GEOS-Chem represents this

with two components: (1) the "balanced biosphere" estimated from the Carnegie-Ames-Stanford-Approach (CASA) model (Potter *et al.*, 1993) with a net annual uptake of 0 PgC/yr to represent the seasonal cycle (2) and the residual annual terrestrial exchange, which was obtained by inverse modeling in the Trans-Com 3 project (Baker *et al.*, 2006) and then adjusted to remove the contribution for biomass burning. Fig. 1 shows the seasonal contrast of net ecosystem exchange (NEE) in 2000 calculated from CASA model. The CO_2 ocean fluxes are from Takahashi *et al.* (2009) with monthly variations, which are based on the 3,000,000 non-El Niño measurements of the pressure of CO_2 dissolved in ocean water. The ocean exchange at sea surface gives a global annual net CO_2 flux of -1.4 PgC/yr, indicating that the ocean is a large sink.

Additional fossil fuel emissions from international shipping (~0.20 PgC/yr) and aviation (~0.16 PgC/yr) are also included. Although these are minor in comparison to the main fossil fuel inventory (~8 PgC/yr), they impact the latitudinal and vertical CO_2 gradients in the atmosphere. CO_2 from the oxidation of other carbon species (~1.05 PgC/yr) makes a larger contribution and has larger impacts on the global 3-D distribution of CO_2 (Nassar *et al.*, 2010). The details of the CO_2 module and the source/sink inventories (including a surface correction for the CO_2 source from oxidation) are explained at Nassar *et al.* (2010). We initially set a uniform global CO_2 concentration on January 1st as 370 ppmv, which is 5 ppmv smaller than Nassar *et al.* (2010) based on the measurements of marine surface mean CO_2 concentration (NOAA-ESRL-GMD sites). But we scaled the global CO_2 distribution pattern in January 2010 after 6 year initialization which gives more realistic initial CO_2 distribution in the atmosphere.

4. RESULTS

4.1 The GOSAT CO₂ Data

We used GOSAT (FTS SWIR, L2) CO_2 products from versions 01.11-0.1.13. Fig. 2 shows the CO_2 column-averaged dry air mole fraction or concentration in each season. This quantity is commonly referred to as XCO_2 and is determined by taking the ratio of the retrieved CO_2 column density to the dry air column density which is retrieved using the O_2 A-band (0.76 µm).

Continental observations of XCO_2 are made in nadir mode and show a pattern of seasonal variation similar to that from the NOAA-ESRL-GMD (http://www. esrl. noaa.gov/gmd/ccgg/trends/#global), where the global marine surfacemean CO_2 level in January 2004 is 377 ppmv. The oceanic XCO_2 values are derived from GOSAT measurements using sun glint mode (Yoshida *et al.*, 2011) and are mostly between 375-380 ppmv (Fig. 2). The hemispheric gradient of CO_2 concentration is observed, but is found to be less than the gradient of *in-situ* or ground measurements, which is expected for column-averaged observations. The relatively low CO_2 level below 375 ppmv over the terrestrial biosphere in the northern hemisphere summer (i.e., North America and Siberia) is evident in Fig. 2. Despite these reasonable distributions in GOSAT data, the limited spatial coverage due to observations excluded by cloud and aerosol filtering is one of the major limita-
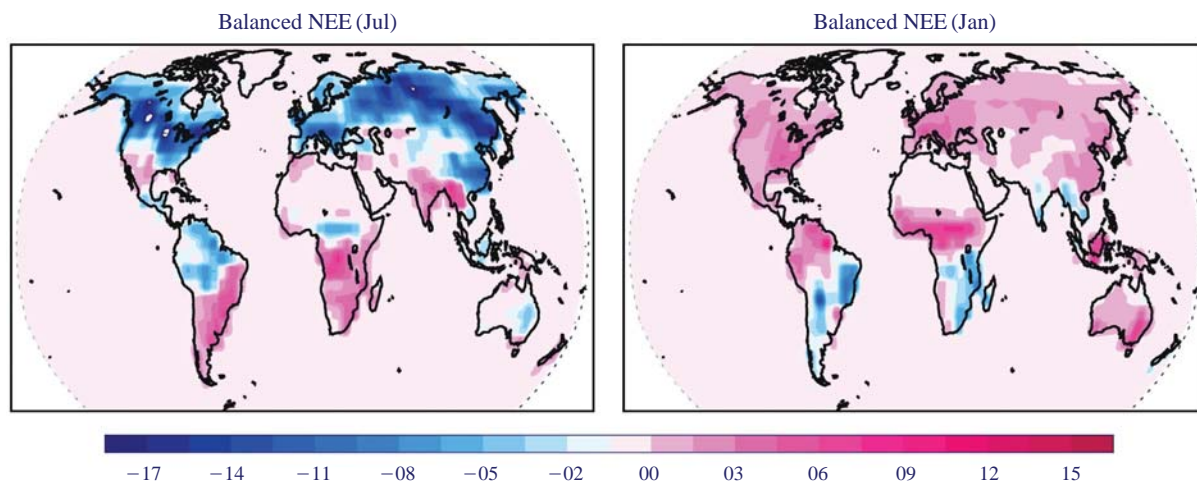

Fig. 1. The monthly "balanced" net ecosystem exchange (NEE) from the CASA model run used in GEOS-Chem, which gives no global net annual CO_2 flux. The left shows the global NEE distribution in July 2000 and the right shows the NEE in January 2000 (unit: 10^{13} molecules/cm²/s).
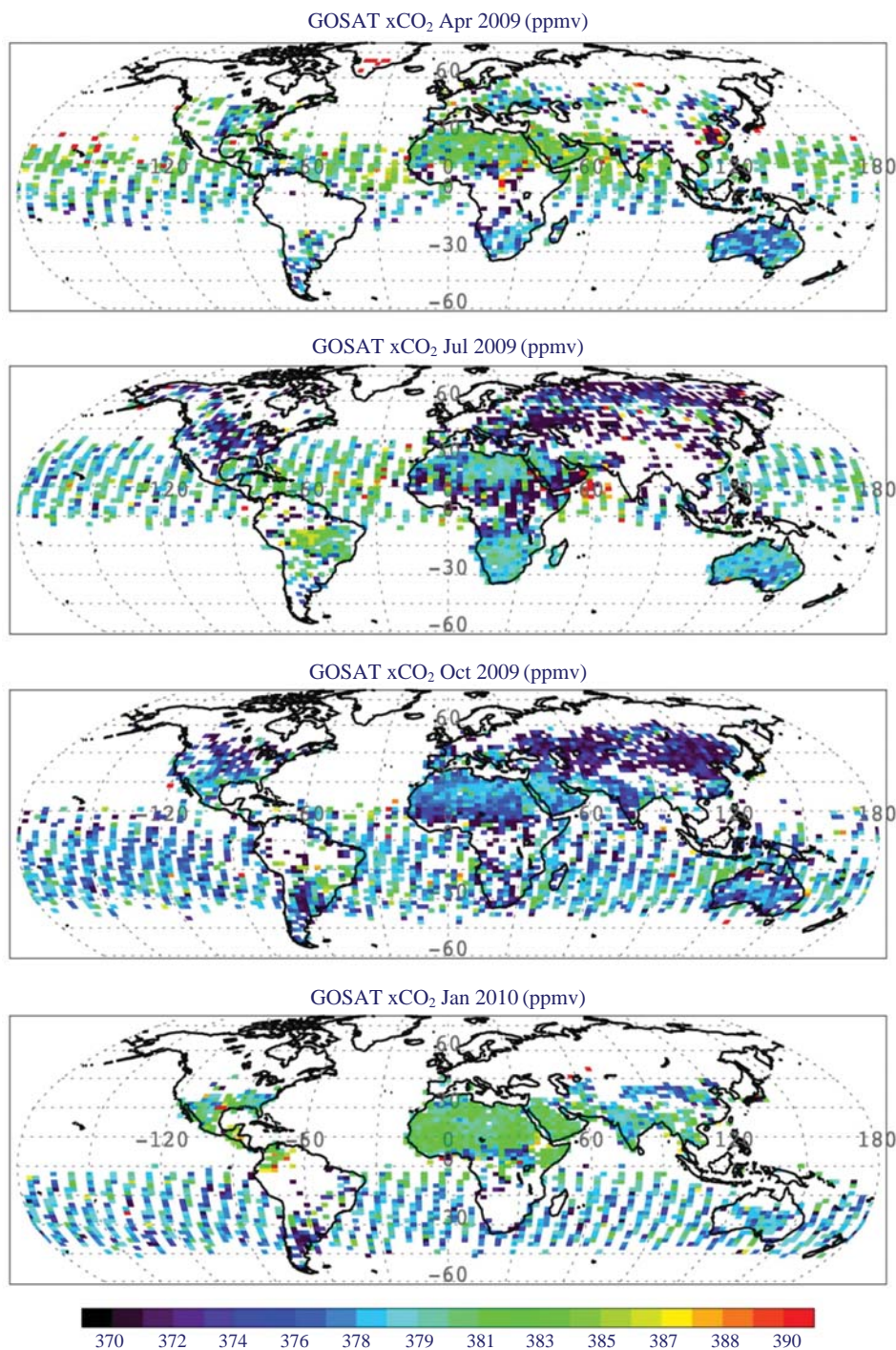
GOSAT xCO$_2$ Apr 2009 (ppmv)

GOSAT xCO$_2$ Jul 2009 (ppmv)

GOSAT xCO$_2$ Oct 2009 (ppmv)

GOSAT xCO$_2$ Jan 2010 (ppmv)

370 372 374 376 378 379 381 383 385 387 388 390

Fig. 2. The seasonal variability in column-averaged CO$_2$ concentration (xCO$_2$) from GOSAT L2 products (April 2009 to January 2010, unit: ppmv).

tions of the product.

4. 2 Comparisons between GOSAT and GEOS-Chem CO$_2$ Data

We compared the total CO$_2$ column densities (unit:

10^{21} molecules/cm^2) between GOSAT and GEOS-Chem data from April 2009 and January 2010, which is shown in Table 1. The comparison between total columns does not consider the averaging kernels of GOSAT data which limits our results from being a

truly quantitative validation. We do not include May, November, and December in 2009 since there were serious data exclusions ($<$5% available) due to the cloud and aerosol interference. Table 1 shows the monthly variation of total CO$_2$ columns over 6 continental regions (East Asia, Europe, North America, Africa, South America, and Australia). In general, the total CO$_2$ column varies between 7.0-9.0×10^{21} molecules/cm^2 and both of the data clearly reproduce the seasonal variation of CO$_2$ (Table 1). GEOS-Chem columns typically have a positive bias of 0.6-1.5% (Table 1). The only exception of GEOS-Chem negative bias occurred over East Asia in April 2009 and January 2010 where the GOSAT CO$_2$ level is slightly higher than the model (Table 1), with the GOSAT columns showing the largest seasonal variability over this region (4.4×10^{20} molecules/cm^2) while GEOS-Chem has a much smaller seasonality (2.4×10^{20} molecules/cm^2). Considering the generally underestimated GOSAT data, these higher GOSAT CO$_2$ concentrations over East Asia in the cold seasons are exceptional. The possible reasons are (1) the anthropogenic CO$_2$ emission over China in the model is still underestimated during these months due to use of an annual mean fossil fuel and cement inventory (the strong NO$_x$ seasonality by fossil fuel use over China is also well shown in satellite-based NO$_2$ data (Lamsal *et al.*, 2010)); (2) Biomass burning emissions for 2009-2010 were not available in GFED2 so, regional interannual differences in those years could lead to lower CO$_2$ in the simulation; (3) anomalously low photosynthetic uptake in the region due potentially to climate perturbations like the onset of El Niño in spring 2009; (4) Model transport errors over Asia or neighboring regions; (5) Measurement interference by Asian dust over East Asia (Yokota *et al.*, 2009).

The column concentrations of the model and GOSAT are largest over Europe (8.02 and 7.96×10^{21} molecules/cm^2, respectively) revealing the latitudinal gradient of CO$_2$ that shows the higher CO$_2$ concentration in the high northern latitudes. GEOS-Chem has a positive bias by ~0.8% but the correlation is relatively poor ($R^2 = 0.33$) which may be due to the very limited GOSAT data sampled over the higher latitudes in the cold season or imperfections in the CO$_2$ flux inventories, thus the estimation of the bias over Europe is more uncertain.

The correlation between GOSAT and GEOS-Chem columns are highest over North America ($R^2 = 0.72$) which may indicate relatively more accurate CO$_2$ flux information over this region than that of the rest of the world. GEOS-Chem has ~1.0% bias and almost the same magnitude of seasonal variation between the two data sets (3.9×10^{20} molecules/cm^2), which is

Table 1. The monthly mean, bias, and correlation of GOSAT and GEOS-Chem CO$_2$ total columns (unit: 10^{21} molecules/cm^2).

	GOSAT	GEOS-Chem	Model bias (%)	R^2
E. Asia				
2009/04	8.127 ± 0.39	8.024 ± 0.36	-1.28	0.40
2009/06	7.836 ± 0.4	7.968 ± 0.38	1.65	0.58
2009/07	7.784 ± 0.4	7.871 ± 0.44	1.12	0.76
2009/08	7.690 ± 0.45	7.786 ± 0.44	1.24	0.74
2009/09	7.722 ± 0.47	7.780 ± 0.44	0.75	0.81
2009/10	7.721 ± 0.52	7.803 ± 0.43	1.05	0.61
2010/01	7.980 ± 0.49	7.937 ± 0.48	-0.53	0.59
Mean			0.57	
Europe				
2009/04	8.091 ± 0.21	8.098 ± 0.26	0.08	0.18
2009/06	7.988 ± 0.35	8.034 ± 0.28	0.57	0.10
2009/07	7.847 ± 0.37	7.918 ± 0.33	0.89	0.36
2009/08	7.831 ± 0.31	7.929 ± 0.3	1.24	0.34
2009/09	7.917 ± 0.23	8.009 ± 0.29	1.15	0.27
2009/10	7.844 ± 0.41	7.929 ± 0.4	1.08	0.38
2010/01	8.171 ± 0.13	8.201 ± 0.3	0.37	0.81
Mean			0.76	
N. America				
2009/04	7.938 ± 0.43	8.008 ± 0.47	0.88	0.64
2009/06	7.836 ± 0.43	7.923 ± 0.5	1.11	0.72
2009/07	7.753 ± 0.46	7.834 ± 0.54	1.03	0.79
2009/08	7.773 ± 0.44	7.856 ± 0.5	1.07	0.74
2009/09	7.650 ± 0.46	7.731 ± 0.54	1.05	0.77
2009/10	7.547 ± 0.51	7.610 ± 0.58	0.83	0.74
2010/01	7.675 ± 0.64	7.752 ± 0.66	0.99	0.69
Mean			0.99	
Africa				
2009/04	7.390 ± 0.42	7.502 ± 0.47	1.50	0.46
2009/06	7.435 ± 0.36	7.484 ± 0.38	0.66	0.48
2009/07	7.479 ± 0.36	7.557 ± 0.4	1.03	0.58
2009/08	7.494 ± 0.42	7.610 ± 0.43	1.53	0.53
2009/09	7.588 ± 0.43	7.707 ± 0.44	1.54	0.58
2009/10	7.675 ± 0.51	7.814 ± 0.48	1.78	0.58
2010/01	7.740 ± 0.46	7.858 ± 0.41	1.5	0.69
Mean			1.36	
S. America				
2009/04	7.765 ± 0.59	7.947 ± 0.46	2.29	0.31
2009/06	7.784 ± 0.65	7.918 ± 0.54	1.7	0.15
2009/07	7.800 ± 0.49	7.879 ± 0.53	1.03	0.16
2009/08	7.806 ± 0.48	7.873 ± 0.54	0.85	0.44
2009/09	7.855 ± 0.36	7.910 ± 0.51	0.69	0.17
2009/10	7.841 ± 0.46	7.959 ± 0.47	1.48	0.15
2010/01	7.855 ± 0.37	7.944 ± 0.47	1.12	0.17
Mean			1.31	
Australia				
2009/04	7.882 ± 0.18	7.981 ± 0.17	1.23	0.44
2009/06	7.922 ± 0.17	7.992 ± 0.16	0.87	0.41
2009/07	7.942 ± 0.16	8.013 ± 0.16	0.90	0.52
2009/08	7.928 ± 0.16	8.013 ± 0.16	1.06	0.58
2009/09	7.932 ± 0.18	8.026 ± 0.17	1.16	0.52
2009/10	7.975 ± 0.18	8.080 ± 0.18	1.30	0.61
2010/01	7.968 ± 0.16	8.056 ± 0.18	1.09	0.58
Mean			1.09	
Continental Mean			1.01	

driven primarily by vegetation activities since GEOS-Chem here used the annual mean fossil fuel emission inventory.

We excluded the region of Saharan desert during the investigation of Africa because the desert storms seriously interfere with the CO_2 retrievals. The seasonal trends show a typical southern hemispheric pattern and the bias is as large as 1.4% (Table 1). The CO_2 concentration over Africa is lowest (7.5-7.6 × 10²¹ molecules/cm²).

In South America, the GEOS-Chem trends do not reproduce the southern hemispheric CO_2 trends which is shown by GOSAT data (Table 1) and the correlation is poor ($R^2=0.21$) with the large bias (~1.3%). This could be attributed to seasonal cycle of CO_2 fluxes coming from the CASA run or the residual annual climatology, which recent inverse modeling work suggested overestimated South American biospheric emissions for 2006 (Nassar *et al.*, 2011). The tropical biosphere shows lower seasonality (0.9 × 10²⁰ molecules/cm²), but we also have to consider the significant number of missing data due to the clouds and aerosols over the Amazon region during the wet season. The data coverage of GOSAT is relatively better over Australia and modeled and GOSAT data show a typical southern hemispheric CO_2 trend (Table 1) with the smaller seasonality (1.0 × 10²⁰ molecules/cm²). The GEOS-Chem bias is closer to the global mean (~1.0%) over Australia. The spatial variance of CO_2 data over Australia is smallest (1.5 × 10²⁰ molecules/cm²), which implies that there are no strong sinks or sources in this region.

The spatial distribution of the differences between GOSAT and GEOS-Chem CO_2 total columns in summer and winter seasons are shown in Figs. 3 and 4. In July 2009, the GEOS-Chem total columns of CO_2 are slightly higher, particularly over the ocean, which gives systemic overestimation by ~8.8 × 10¹⁹ molecules/cm². The global mean difference here is ~1.0% and the spatial pattern is reasonably comparable between two data sets with the correlation ($R^2=0.6$). This difference is entirely consistent with the ~1.0% bias determined by from the 7 months of observations assuming equal-weighting of the continents (Table 1). The value is slightly larger than the mean GOSAT uncertainties (<1%) reported by Yoshida *et al.* (2011).

4. 3 Comparison with WDCGG CO_2 Data

Previously, a global GEOS-Chem CO_2 simulation was compared with the data from 74 GLOVALVIEW-CO_2 sites by Nassar *et al.* (2010). Although direct comparisons of this type have limitations due to the representation error caused by the size mismatch between the model domain and sites, the GEOS-Chem CO_2 generally agreed well with GLOBALVIEW-CO_2 data (Nassar *et al.*, 2010). With the same limitation but different initial conditions, we focused on the comparison of the monthly mean GEOS-Chem CO_2 with ground-based measurements from 12 sites, available from the World Data Center for Greenhouse Gases (WDCGG) (WMO, 2009) from January 2004 to December 2009. The sites selected represent a range of latitudes and different regions, with most being remote background sites. However, the two Korean sites (Taeahn (36.72° N, 126.12° E) and Gosan (33.17° N, 126.1° E)), Jungfraujoch (45.5° N, 8° E), and Sable Island (43.9° N, 60° W) are somewhat closer to the industrial areas of China, Europe, and North America. The model comparison with the ground-based data is important to help infer the quality of the GOSAT CO_2 products since the vertically-integrated GOSAT column data cannot be compared directly with the ground-based "point" measurements. The fact that the model simulates a complete 3-D field allows it to be compared with both measurement approaches.

During the comparison, we first calculated the GEOS-Chem biases which have a range from −1.5% to −0.5% and corrected the model bias by adding the mean bias (3.6 ppmv) for the 12 sites. Correction with a fixed value does not change the correlation between the model and observation data. The red lines in Fig. 5 indicate the model data with the bias correction and black dots shows the observations. As shown in Fig. 5, the GEOS-Chem simulations represent the seasonal cycle of the observation timeseries very well, resulting in a fairly high correlation range ($0.66 \le R^2 \le 0.99$).

The large gradient of the seasonal variability of CO_2 with latitude is shown in Fig. 5. The comparison for the remote stations shows high correlations with the GEOS-Chem data ($R^2>0.90$). Jungfraujoch, Taeahn, and Gosan had relatively lower correlations (0.66-0.75), which likely relates to their inland locations and proximity to industrial sources or natural terrestrial flux regions, which are challenging to model, or from the impact of representativeness errors. The sites of East Asia (Taeahn and Gosan) have a large seasonal variability (>15 ppmv) due to the strong continental influence, which is not captured very well by the model (Fig. 5). The high correlation at Sable Island may imply that the CO_2 fluxes or model transport over North America are better represented in the model than for other continents.

The GEOS-Chem data without the correction on Taeahn and Gosan show 0.6%-1.6% negative bias that is particularly larger during the winter and spring season. That large discrepancy may be due in part to the fact that the GEOS-Chem simulation used the annual
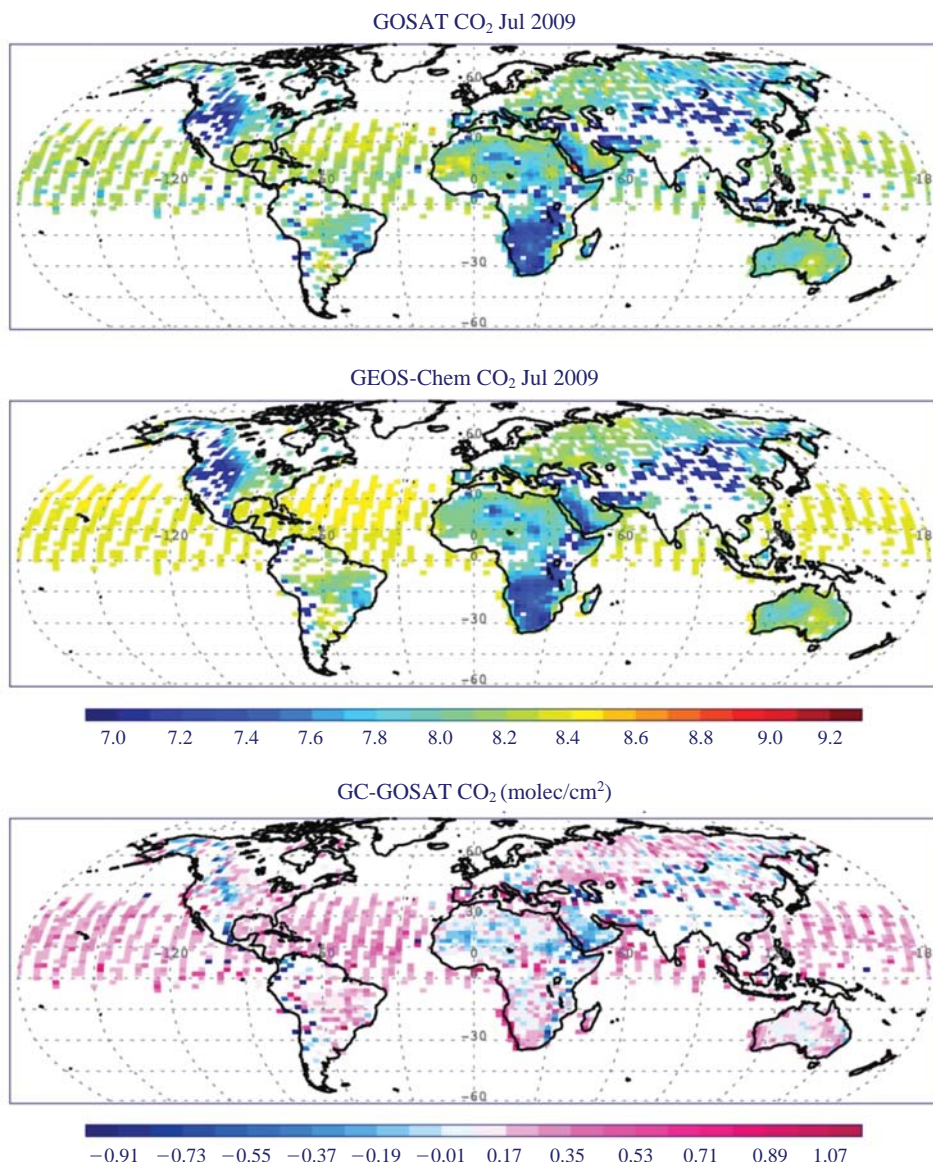
GOSAT CO$_2$ Jul 2009

GEOS-Chem CO$_2$ Jul 2009

| 7.0 | 7.2 | 7.4 | 7.6 | 7.8 | 8.0 | 8.2 | 8.4 | 8.6 | 8.8 | 9.0 | 9.2 |

GC-GOSAT CO$_2$ (molec/cm^2)

| −0.91 | −0.73 | −0.55 | −0.37 | −0.19 | −0.01 | 0.17 | 0.35 | 0.53 | 0.71 | 0.89 | 1.07 |

Fig. 3. The monthly average of GOSAT CO$_2$ column density in July 2009 (top), the corresponding GEOS-Chem data (middle) and the difference between GEOS-Chem and GOSAT CO$_2$ column density (GEOS-Chem-GOSAT) (bottom: unit: 10^{21} molecules/cm^2).

mean anthropogenic CO$_2$ emission inventory that averaged out the seasonal anthropogenic CO$_2$ trends of China, resulting in the seasonal difference in the bias (~11 ppmv in the winter and ~2.5 ppmv in the summer for the Korean sites) and due in part to the lower initial condition for the CO$_2$ (January 2004) than applied in Nassar et al. (2010).

Based on the comparison with those global ground measurements, GEOS-Chem data reproduce the observed CO$_2$ data well with a systemic bias (3.6 ppmv or ~1.0%) and we can infer that the GOSAT data have a negative bias of ~2.0%, which is consistent with the

recent validation study of Morino et al. (2011) that compared the NIES XCO$_2$ with ground-based FTS XCO$_2$ measurements from the Total Carbon Column Observing Network (TCCON, Wunch et al., 2010) and found a low bias of 8.85 ± 4.75 ppm ($2.3 \pm 1.2\%$). Another major L2 GOSAT dataset has been developed by the NASA-led Atmospheric Carbon Observations from Space (ACOS) team using a different retrieval algorithm (O'Dell et al., 2011) on the same observations. Wunch et al. (2011) compared the ACOS-GOSAT retrievals to TCCON and found a low bias of 1.8%, which they attribute to multiple sources. Retrie-

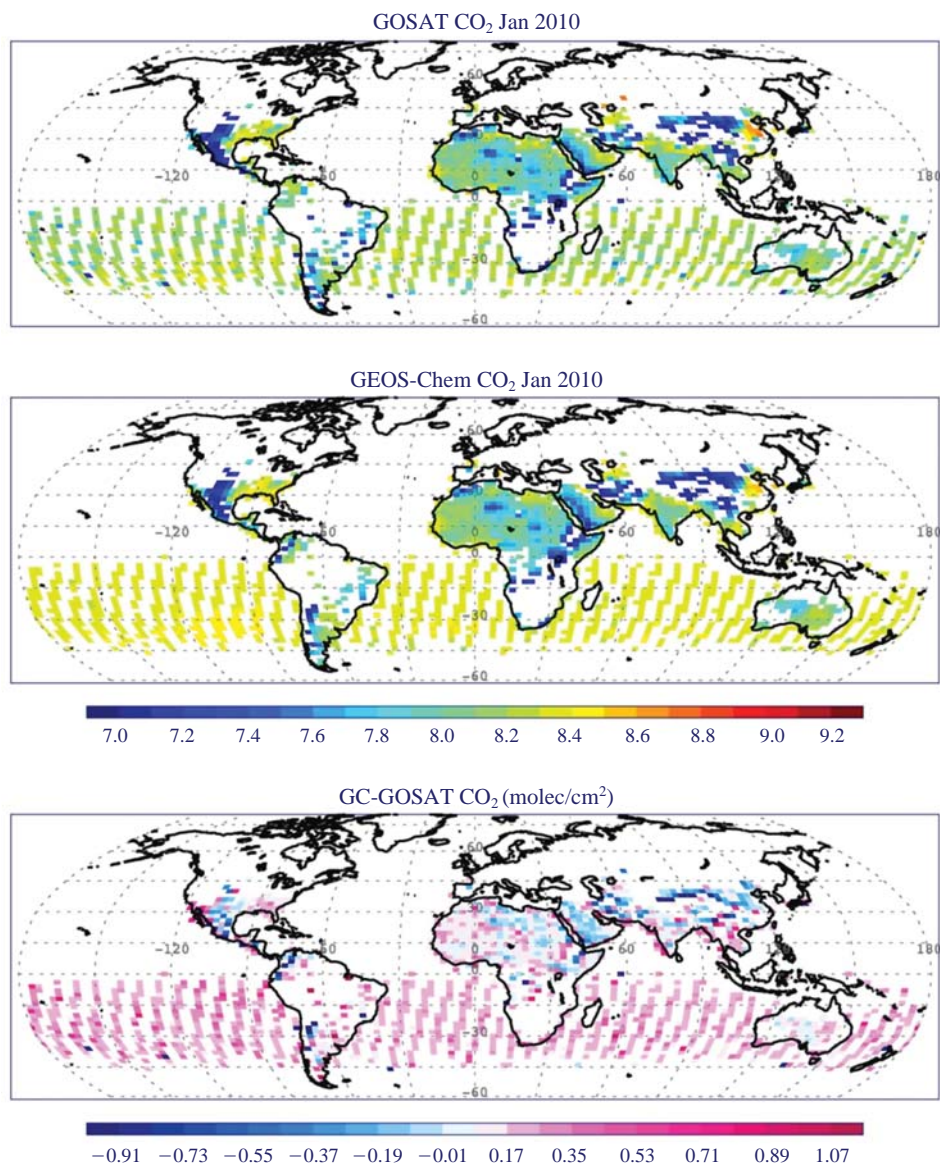GOSAT CO_2 Jan 2010

GEOS-Chem CO_2 Jan 2010

GC-GOSAT CO_2 (molec/cm^2)

Fig. 4. Same as Fig. 3, but in January 2010.

val of GOSAT data by another team (Butz *et al.*, 2011) corrected for a 3% bias in the O_2 A-band, which they identify as the primary source of the XCO_2 bias in cloud-free observations, such that after the correction, the XCO_2 bias for cloud-free observations was only −0.05% relative to TCCON. It should be noted that a different empirical correction approach is used to correct the TCCON ground-based FTS XCO_2 data for presumed biases (Wunch *et al.*, 2010). If the source of the GOSAT XCO_2 bias overall is predominantly due to the O_2 A-band, as suggested by Butz *et al.* (2011) based on an analysis of cloud-free observations, then overall GOSAT CO_2 column densities should only have

minor biases perhaps due to retrievals with low levels of cloud and aerosol, that were not excluded based on the CAI data and other screening methods. Until the entire cause of the GOSAT bias can be definitely confirmed, evaluation and comparison of GOSAT L2 CO_2 products using a number of different methods (TCCON, model-based approaches, etc.) will be important.

4. 4 Contributions of Sources/Sinks to Atmospheric CO_2

We estimated each source/sink contribution to the global atmospheric CO_2 budget using a tagged CO_2 simulation in which the each source/sink is treated as
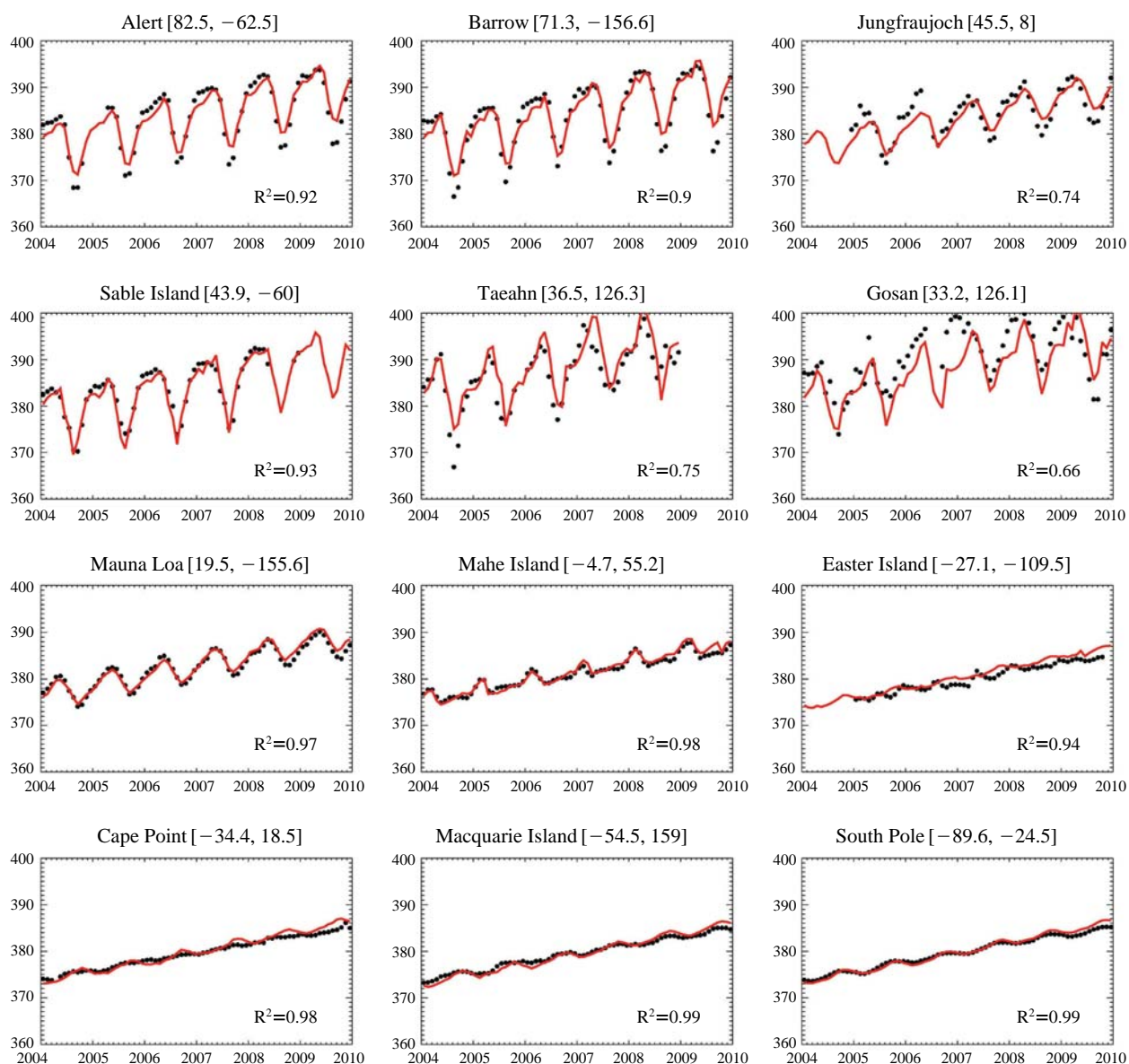
Fig. 5. The comparison of CO$_2$ data between 12 ground-based measurement sites from WDCGG (black) and GEOS-Chem (red). The model data have been adjusted here by correcting them with the average GEOS-Chem bias from 12 sites (3.6 ppmv).

an individual tracer. The tagged simulation is useful since the geographically defined state vector can be applied for inverse modeling (Nassar *et al.*, 2011) to constrain the surface CO$_2$ fluxes and the spatial distribution and trends of each source/sink's contribution can be understood. This calculation of the source/sink contribution to atmospheric CO$_2$ can provide useful information for greenhouse gas reduction targets and strategies for policy-makers. Here the tagged simulation estimated the individual source/sink contribution to the global atmospheric CO$_2$ concentration (ppmv)

for 6 recent years (January 2004 to December 2009, Figs. 6-10). The tagged simulation results show the spatial and vertical distributions of each contribution. Table 2 represents the accumulated source/sink contributions over the 6-year period in terms of the global CO$_2$ budget and annual trends.

Fig. 6 represents the global atmospheric CO$_2$ contribution by fossil fuel and cement production. The globally-averaged accumulated contribution is about 19.5 ppmv for the 6 year period (2004-2009). There is a significant latitudinal gradient in the contribution
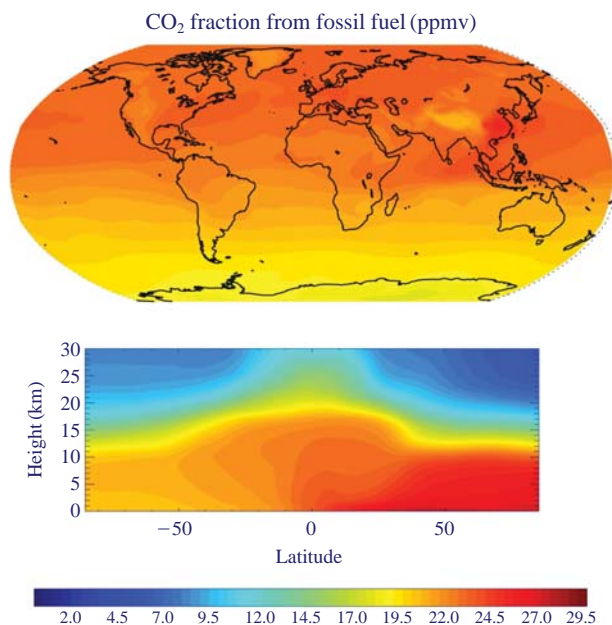
CO$_2$ fraction from fossil fuel (ppmv)

Fig. 6. The column-averaged CO$_2$ fraction (unit: ppmv) contributed by fossil fuel combustion and cement production from a tagged GEOS-Chem simulation for January 2004 and December 2009.
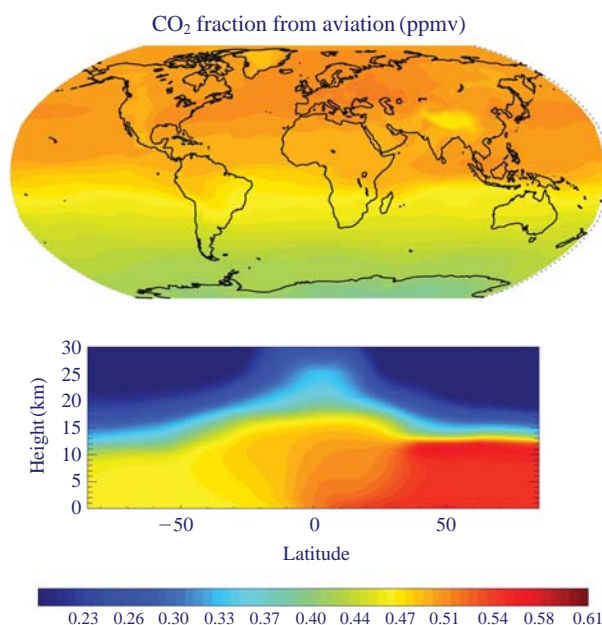
CO$_2$ fraction from aviation (ppmv)

Fig. 8. Same as Fig. 6, but for the contribution from aviation.

CO$_2$ fraction from Biomass Burning (ppmv)
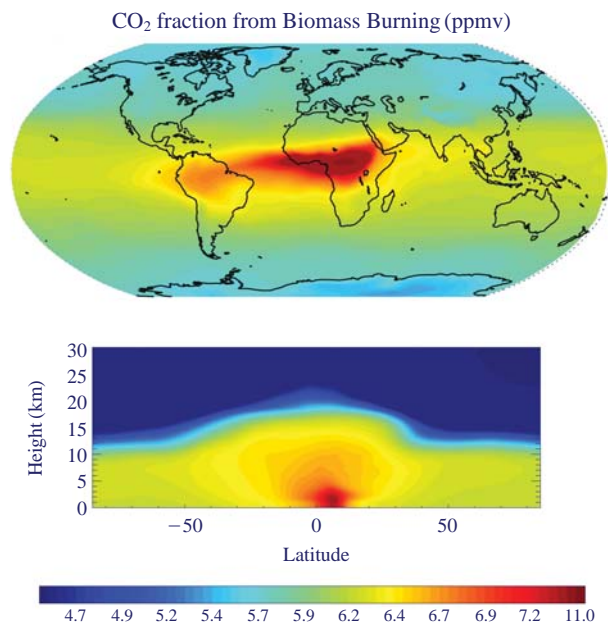
Fig. 7. Same as Fig. 6, but for the contribution from biomass burning.

CO$_2$ fraction from terrestiral biosphere (ppmv)

Fig. 9. Same as Fig. 6, but for the contribution from the terrestrial biosphere (net terrestrial exchange).

that is particularly strong due to the large emissions from E. Asia and E. US despite inter-hemispheric transport (Fig. 6). The emission of CO$_2$ from biomass burning is largest in the tropics (Africa, Amazonia, Indonesia) and the contribution to atmospheric CO$_2$ is thus stronger within the tropical regions (>6.0 ppmv for 6 years, Fig. 7). GEOS-Chem used a 3-D emission inventory for aviation that is dominant in the inter-

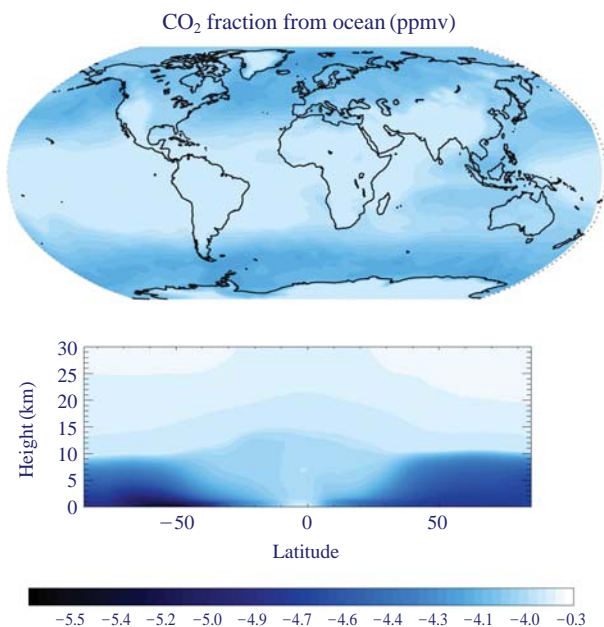CO₂ fraction from ocean (ppmv)

Fig. 10. Same as Fig. 6, but for the contribution from oceanic exchange.

continental airline contrails such as over the N. Atlantic and N. Pacific regions. The influence is shown in Fig. 8. The contribution spreads throughout troposphere and low stratosphere due to the flight paths of commercial aircraft.

The tagged CO_2 simulation calculated the contribution of the residual annual terrestrial exchange (-13.3 ppmv/6 years), which is higher in the northern hemisphere due to the larger fraction of the continents and hence terrestrial vegetation (Fig. 9). Since these fluxes were based on inversions using the standard 11 Transcom land regions (Baker *et al.*, 2006) they contain very limited information on sources/sinks at sub-continental scales. Regional scale information of net ecosystem exchange based on measurements needs to be applied to more precisely to understand the atmospheric CO_2 budget. Fig. 10 represents the spatial distribution of the oceanic contribution that is mostly influenced by the sea surface sinks at the high latitudes (>3.0 ppmv).

The mean global trend of CO_2 based on the measurements has been growing (Keeling *et al.*, 1995) from ~1.5 ppmv/year during the 1980s to the early 1990s (Conway *et al.*, 1994) to ~1.8 ppmv/year from 1993 to 2005 (Matsueda *et al.*, 2008). The recent satellite CO_2 retrievals from the NASA's Atmospheric InfraRed Sounder (AIRS) have been recently validated with aircraft data and the annual mean growth rate in the middle troposphere is 1.98 ppmv/year from 2002 to 2008 (Olsen *et al.*, 2008).

The GEOS-Chem generally reproduces the observed trend of global atmospheric CO_2 (2.08 ppmv/year) and the simulated global CO_2 increase from 2004 to 2009 is shown in Fig. 11. This interannual trend is mainly driven by the national fossil fuel combustion inventory (3.2 ppmv/year, Table 2), which includes a contribution from cement manufacture of ~2-5%. Net terrestrial and oceanic exchange of CO_2 are the main sinks (-2.2 ppmv/year and -0.6 ppmv/year, respectively, Table 2). Thus it is clear that a large reduction to the human contribution to the carbon cycle is required to limit the current global atmospheric CO_2 increase. However, there are still many unknowns that could be better understood regarding the atmospheric CO_2 budget, which could help to achieve emission reduction targets. Carbon exchange in the terrestrial biosphere (and to some extent the ocean) tends to have relatively large spatiotemporal variability, which is one of the key questions to better estimate the global CO_2 budget. The influence of the atmospheric transport including El Niño/Southern Oscillation (ENSO) events also needs to be quantitatively understood.

5. CONCLUSIONS

Here we simulated CO_2 concentrations with a global 3-D chemical transport model (GEOS-Chem) and compared the model results with recently available GOSAT satellite observations from April 2009 to January 2010. We found that GEOS-Chem total CO_2 columns overestimated the GOSAT data by ~1.0% with a reasonable agreement in the spatial distribution, but there is a significant continental dependence in those agreements. The highest agreement over North America perhaps indicate the best source/sink information based on the intense measurements and study over many years. Larger biases and poor correlations over Africa, South America and Europe might indicate limitations in model inventories and atmospheric transport. After correcting for the systematic underestimation of CO_2 in GEOS-Chem data with the global ground-based measurements from WDCGG, a ~2.0% negative bias in GOSAT CO_2 is inferred.

The unusual negative model bias with GOSAT over East Asia during the cold season and the larger negative model bias with the Korean stations may suggest that Chinese emission of CO_2 from fossil fuel combustion exceeds the inventory values and has a relatively large seasonality. The monthly emission inventory of fossil fuel combustion and cement production by Andreas *et al.* (2011), recently became publicly available and will be implemented in a future study that will be more focused on the East Asian regions
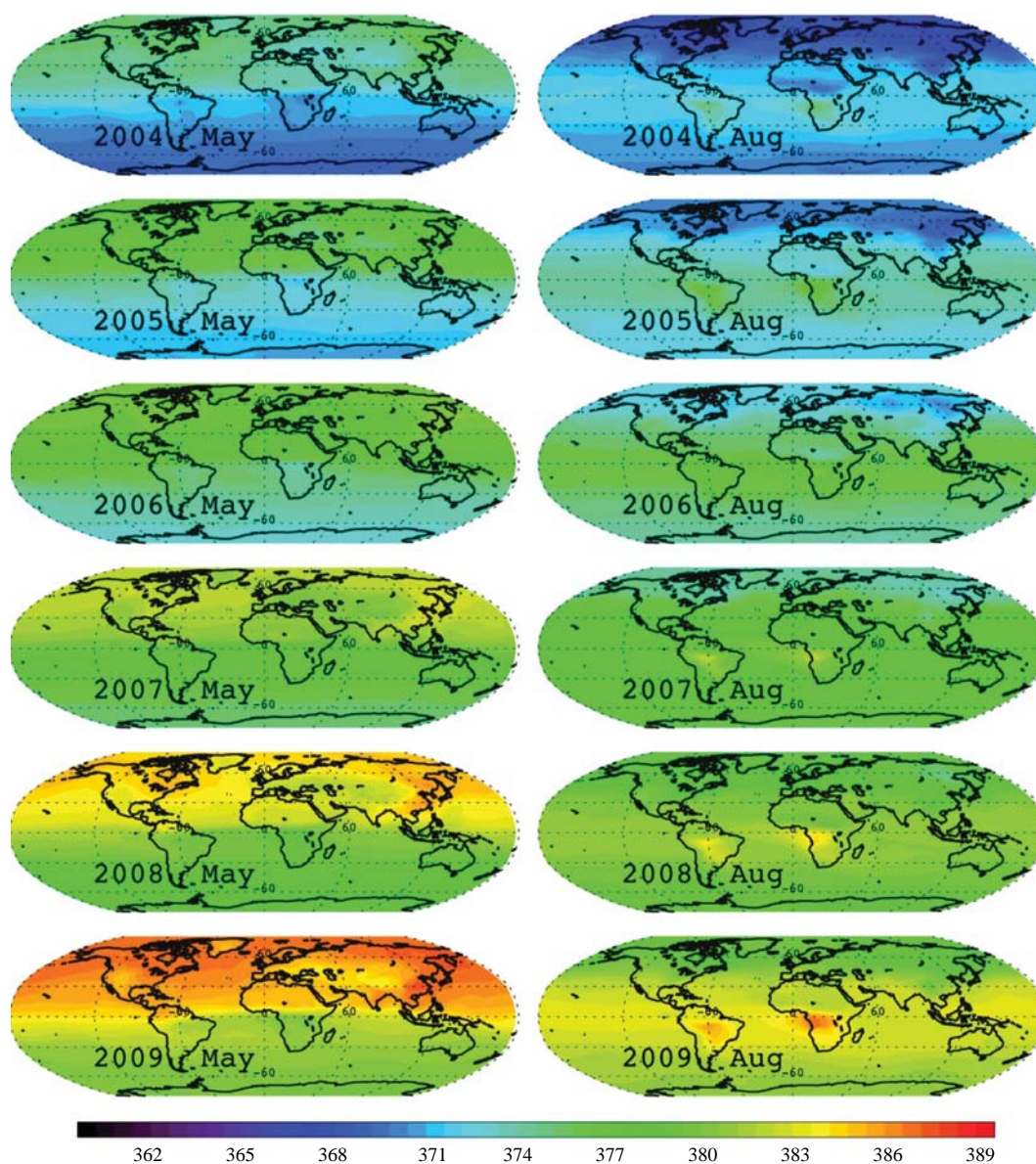
Fig. 11. The global column-averaged CO_2 concentration simulated by GEOS-Chem model from 2004 to 2009, demonstrating the seasonal cycle and annual increase.

Table 2. The source/sink contributions to global CO_2 concentration and annual trends from 2004-2009.

	FF	OC	BB	BF	NTE	SHIP	AVI	Chem	Corr	Total
Contribution (ppmv)	19.5	−3.6	5.4	2.1	−13.3	0.5	0.42	2.92	−2.04	11.9
Trends (ppmv/year)	3.2	−0.58	0.88	0.34	−2.17	0.082	0.07	0.48	−0.34	2.08

FF (fossil fuel and cement production), OC (ocean), BB (biomass burning), BF (biofuel burning), NTE (net terrestrial exchange), SHIP (shipping), AVI (aviation), Chem (chemical production), Corr (correction factor)

for a quantitative comparison with satellite and *in-situ* observations. Subsequent versions of the GOSAT retrievals are addressing the current negative bias as well as the problem of massive data exclusion due to cloud and aerosol detection, which will enhance the overall quality of the data.

Although the atmospheric CO_2 lifetime is approximately a century, our tagged CO_2 simulation for a 6-year run (2004-2009) shows that most of sources and sinks have spatial gradients to their CO_2 contributions. Human-induced emission from fossil fuel combustion and cement production is likely to be a main driving force to accelerate the current CO_2 trends, which supports the international efforts to reduce the anthropogenic CO_2 emissions. The information of quantitative CO_2 fraction by each source/sink (e.g., biospheric CO_2 exchanges) is useful to apply the inverse modeling with CO_2 satellite measurements such as GOSAT data will help to better constrain the spatial distribution and efficiency of the individual source/sink, providing important information for CO_2 reduction targets and strategies in the 21st century.

ACKNOWLEDGEMENT

REFERENCES

Andres, R.J., Gregg, J.S., Losey, L., Marland, G., Boden, T.A. (2011) Monthly, global emissions of carbon dioxide from fossil fuel consumption. Tellus 63B, 309-327, doi:10.1111/j.1600-0889.

Baker, D.F., Law, R.M., Gurney, K.R., Rayner, P., Peylin, P., Denning, A.S., Bousquet, P., Bruhwiler, L., Chen, Y.-H., Ciais, P., Fung, I.Y., Heimann, M., John, J., Maki, T., Maksyutov, S., Masarie, K., Prather, M., Pak, B., Taguchi, S., Zhu, Z. (2006) TransCom 3 inversion intercomparison: impact of transport model errors on the intercontinental variability of regional CO_2 fluxes, 1988-2003. Global Biogeochemical Cycle 20, GB1002, doi:10.1029/2004GB002439.

Bey, I., Jacob, D.J., Yantosca, R.M., Logan, J.A., Field, B.D., Fiore, A.M., Li, Q., Liu, H.Y., Mickley, L.J., Schultz, M.G. (2001) Global modeling of tropospheric chemistry with assimilated meteorology: Model description and evaluation. Journal of Geophysical Research 20,106(D19), 23073-23095.

Buchwitz, M., Schneising, O., Burrows, J.P., Bovens-
mann, H., Reuter, M., Notholt, J. (2007) First direct observation of the atmospheric CO_2 year-to-year increase from space. Atmospheric Chemistry and Physics 7, 4249-4256.

Butz, A., Guerlet, S., Hasekamp, O., Shepers, D., Galli, A., Aben, I., Frankenberg, C., Hartmann, J.M., Tran, A., Kuze, A., Keppel-Aleks, G., Toon, G., Wunch, D., Wennberg, P., Deutscher, N., Griffith, D., Macatangay, R., Messerschmidt, J., Notholt, J., Warneke, T. (2011), Toward accurate CO_2 and CH_4 observations from GOSAT. Geophysical Research Letters 38, L14812, doi:10.1029/2011GRL047888.

Chahine, M.T., Chen, L., Dimotakis, P., Jiang, X., Li, Q., Olsen, E.T., Pagano, T., Randerson, J., Yung, Y.L. (2008) Satellite remote sounding of mid-tropospheric CO_2. Geophysical Research Letters 35, L17807, doi: 10.1029/2008GL035022.

Chevallier, F., Engelen, R.J., Carouge, C., Conway, T.J., Peylin, P., Pickett-Heaps, C., Ramonet, M., Rayner, P.J., Xueref-Remy, I. (2009) AIRS-based versus flask-based estimation of carbon surface fluxes. Journal of Geophysical Research 114, D20303, doi:10.1029/2009 JD012311.

Chevallier, F., Fisher, M., Peylin, P., Serrar, S., Bousquet, P., Bréon, F.-M., Chédin, A., Ciais, P. (2005) Inferring CO_2 sources and sinks from satellite observations: Method and application to TOVS data. Journal of Geophysical Research 110, D24309, doi:10.1029/ 2005JD006 390.

Conway, T.J., Tans, P.P., Waterman, L.S., Thoning, K.W., Kitzis, D.R., Masarie, K.A., Zhang, N. (1994) Evidence for interannual variability of the carbon cycle from the National Oceanic and Atmospheric Administration/Climate Monitoring and Diagnostics Laboratory global air sampling network. Journal of Geophysical Research 99, 22831-22855.

Crevoisier, C., Chédin, A., Matsueda, H., Machida, T., Armante, R., Scott, N.A. (2009) First year of upper tropospheric integrated content of CO_2 from IASI hyperspectral infrared observations. Atmospheric Chemistry and Physics 9, 4797-4810.

Kadygrov, N., Maksyutov, S., Eguchi, N., Aoki, T., Nakazawa, T., Yokota, T., Inoue, G. (2009) Role of simulated GOSAT total column CO_2 observations in surface CO_2 flux uncertainty reduction. Journal of Geophysical Research 114, D21208, doi:10.1029/2008JD 011597.

Keeling, C.D., Whorf, T.P., Wahlen, M., Vanderplicht, J. (1995) Interannual extremes in the rate of rise of atmospheric carbon dioxide since 1980. Nature 375, 666-670.

Kulawik, S.S., Jones, D.B.A., Nassar, R., Irion, F.W., Worden, J.R., Bowman, K.W., Machida, T., Matsueda, H., Sawa, Y., Biraud, S.C., Fisher, M., Jacobson, A.R. (2010) Characterization of Tropospheric Emission Spectrometer (TES) CO_2 for carbon cycle science. Atmospheric Chemistry and Physics 10, 5601-5623.

Kuze, A., Urabe, T., Suto, H., Kaneko, Y., Hamazaki, T.

(2006) The instrumentation and the BBM test results of thermal and near-infrared sensor for carbon observation (TANSO) on GOSAT. Proc, SPIE, 6297, Infrared Spaceborne Remote Sensing, XIV.

Lamsal, L.N., Martin, R.V., van Donkelaar, A., Celarier, E.A., Bucsela, E.J., Boersma, K.F., Dirksen, R., Luo, C., Wang, Y. (2010) Indirect validation of tropospheric nitrogen dioxide retrieved from the OMI satellite instrument: insight into the seasonal variation of nitrogen oxides at northern midlatitudes. Journal of Geophysical Research 115, doi:10.1029/2009JD013 351.

Maksyutov, S., Kadygrov, N., Nakatsuka, Y., Patra, P.K., Nakazawa, T., Yokota, T., Inoue, G. (2008) Projected impact of the GOSAT observatio on regional CO_2 flux estimation as a function of total retrieval error. Journal of Remote Sensing Society of Japan 28, 190-197.

Matsueda, H., Machida, T., Sawa, Y., Nakagawa, Y., Hirotani, K., Ikeda, H., Kondo, N., Goto, K. (2008) Evaluation of atmospheric CO_2 measurements from new flask air sampling of JAL airliner observations. Papers in Meteorology and Geophysics 59, 1-17.

Morino, I., Uchino, O., Inoue, M., Yoshida, Y., Yokota, T., Wennberg, P.O., Toon, G.C., Wunch, D., Roehl, C.M., Notholt, J., Warneke, T., Messerschmidt, J., Griffith, D.W.T., Deutscher, N.M., Sherlock, V., Connor, B., Robinson, J., Sussmann, R., Rettinger, M. (2011) Preliminary validation of column-averaged volume mixing ratios of carbon dioxide and methane retrieved from GOSAT short-wavelength infrared spectra. Atmospheric Measurement Techniques 4, 1061-1076.

Nassar, R., Jones, D.B.A., Kulawik, S.S., Worden, J.R., Bowman, K.W., Andres, R.J., Suntharalingam, P., Chen, J.M., Brenninkmeijer, C.A.M., Schuck, T.J., Conway, T.J., Worthy, D.E. (2011) Inverse modeling of CO_2 sources and sinks using satellite observations of CO_2 from TES and surface flask measurements. Atmospheric Chemistry and Physics 11, 6029-6047.

Nassar, R., Jones, D.B.A., Suntharalingam, P., Chen, J.M., Andres, R.J., Wecht, K.J., Yantosca, R.M., Kulawick, S.S., Bowman, K.W., Worden, J.R., Machida, T., Matsueda, H. (2010) Modeling global atmospheric CO_2 with improved emission inventories and CO_2 production from the oxidation of other carbon species. Geoscientific Model Development 3, 689-716.

O'Dell, C.W., Connor, B., Bösch, H., O'Brien, D., Frankenberg, C., Castano, R., Christi, M., Crisp, D., Eldering, A., Fisher, B., Gunson, M., McDuffie, J., Miller, C.E., Natraj, V., Oyafuso, F., Polonsky, I., Smyth, M., Taylor, T., Toon, G.C., Wennberg, P.O., Wunch, D. (2011) The ACOS CO_2 retrieval algorithm-Part 1: Description and validation against synthetic observations. Atmospheric Measurement Techiques Discussions 4, 6097-6158, doi:10.5194/ amtd-4-6097-2011.

Olsen, E.T., Chahine, M.T., Chen, L., Jiang, X., Pagano, T., Yung, Y.L. (2008) Validation of AIRS retrievals of CO_2 via comparison to in situ measurements. EOS Transactions American Geophysical Union 89, A32B-04, Dec 15-19, 2008.

Potter, C.S., Randerson, J.T., Field, C.B., Matson, P.A., Vitousek, P.M., Mooney, H.A., Klooster, S.A. (1993) Terrestrial ecosystem production: a process model based on global satellite and surface data. Global Biogeochemical Cycle 7, 811-841.

Suntharalingam, P., Jacob, D.J., Palmer, P.I., Logan, J.A., Yantosca, R.M., Xiao, Y., Evans, M.J., Streets, D., Vay, S.A., Sachse, G. (2004) Improved quantification of Chinese carbon fluxes using CO_2/CO correlations in Asian outflow. Journal of Geophysical Research 109, D18S18, doi:10.1029/2003JD004362.

Takahashi, T., Sutherland, S.C., Wanninkhof, R., Sweeney, C., Feely, R.A., Chipman, D.W., Hales, B., Friederich, G., Chavez, F., Sabine, C., Watson, A., Bakker, D.C.E., Schuster, U., Metzl, N., Yoshikawa-Inoue, H., Ishii, M., Nidorikawa, T., Nojiri, Y., Körtzinger, A., Steinhoff, T., Hoppema, M., Olafsson, J., Arnarson, T.S., Tilbrook, B., Johannessen, T., Olsen, A., Bellerby, R., Wong, C.S., Belille, B., Bates, N.R., de Baar, H.J.W. (2009) Climatological mean and decadal change in surface ocean pCO_2, and net sea-air CO_2 flux over the global oceans. Deep-Sea Research Pt. II, doi: 10.1016/j.dsr2.2008.12.009.

van der Werf, G.R., Randerson, J.T., Giglio, L., Collatz, G.J., Kasibhatla, P.S., Arellano, A.F. Jr. (2006) Interannual variability in global biomass burning emissions from 1997 to 2004. Atmospheric Chemistry and Physics 6, 3423-3441.

World Meteorological Organization (WMO) (2009) Technical Report of Global Analysis Method for Greenhouse Gases by the World Data Center for Greenhouse Gases.

Wunch, D., Toon, G.C., Wennberg, P.O., Wofsy, S.C., Stephens, B.B., Fischer, M.L., Uchino, O., Abshire, J.B., Bernath, P., Biraud, S.C., Blavier, J.-F.L., Boone, C., Bowman, K.P., Browell, E.V., Campos, T., Conner, B.J., Daube, B.C., Deutscher, N.M., Diao, M., Elkins, J.W., Gerbig, C., Gottlieb, E., Griffith, D.W.T., Hurst, D.F., Jimenez, R., Keppel-Aleks, G., Kort, E.A., Macatangay, R., Machida, T., Matsueda, H., Moore, F., Morino, I., Park, S.J. Robinson, J., Roehl, C.M., Sawa, Y., Sherlock, V., Sweeney, C., Tanaka, T., Zondlo, M.A. (2010) Calibration of the total carbon column observing network using aircraft profile data. Atmospheric Measurement Techniques 3, 1351-1362, doi:10.5194/ amt-3-1351-2010.

Wunch, D., Wennberg, P.O., Toon, G.C., Connor, B.J., Fisher, B., Osterman, G.B., Frankenberg, C., Mandrake, L., O'Dell, C., Ahonen, P., Biraud, S.C., Castano, R., Cressie, N., Crisp, D., Deutscher, N.M., Eldering, A., Fisher, M.L., Griffith, D.W.T., Gunson, M., Heikkinen, P., Keppel-Aleks, G., Kyrö, E., Lindenmaier, R., Macatangay, R., Mendonca, J., Messerschmidt, J., Miller, C.E., Morino, I., Notholt, J., Oyafuso, F.A., Rettinger, M., Robinson, J., Roehl, C.M., Salawitch, R.J., Sherlock, V., Strong, K., Sussmann, R., Tanaka, T., Thompson, D.R., Uchino, O., Warneke, T., Wofsy, S.C. (2011) A method for evaluating bias in glo-

bal measurements of CO$_2$ total columns from space. Atmospheric Chemistry and Physics 11, 10765-10777.

Yevich, R., Logan, J.A. (2003) An assessment of biofuel use and burning of agricultural waste in the developing world. Global Biogeochemical Cycle 17(4), 1095.

Yokota, T., Yoshida, Y., Eguchi, N., Ota, Y., Tanaka, T., Watanabe, H., Maksyutov, S. (2009) Global concentration of CO$_2$ and CH$_4$ retrieved from GOSAT: First Preliminary Results. SOLA 5, 160-163, doi:10.2151/sola.2009-041.

Yoshida, Y., Eguchi, N., Ota, Y., Kikuchi, N., Nobuta, K., Aoki, T., Yokota, T. (2010) Algorithm theoretical basis document (ATBD) for CO$_2$ and CH$_4$ column amounts retrieval from GOSAT TANSO-FTS SWIR. NIES, GOSAT project Document (NIES-GOSAT-PO-014) Version 1.0.

Yoshida, Y., Ota, Y., Eguchi, N., Kikuchi, N., Nobuta, K., Tran, H., Morino, I., Yokota, T. (2011) Retrieval algorithm for CO$_2$ and CH$_4$ column aboundances from short-wavelength infrared spectral observations by the Greenhouse Gases Observing Satellite. Atmospheric Measurement Techniques 4, 717-734, doi:10.5194/amt-4-717-2011.